Accepted Manuscript

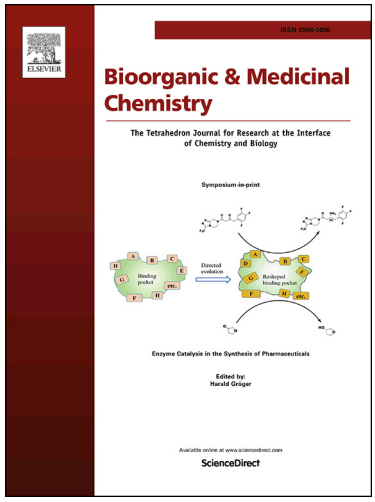

Chemical synthesis and biological activity of novel brominated 7-deazaadenosine-3',5'-cyclic monophosphate derivatives

Marco Lelle, Maik Otte, Susanne Thon, Daniela Bertinetti, Friedrich W. Herberg, Klaus Benndorf

PII: S0968-0896(19)30217-2
DOI: https://doi.org/10.1016/j.bmc.2019.03.024
Reference: BMC 14816

To appear in: *Bioorganic & Medicinal Chemistry*

Received Date: 7 February 2019
Revised Date: 9 March 2019
Accepted Date: 11 March 2019

Please cite this article as: Lelle, M., Otte, M., Thon, S., Bertinetti, D., Herberg, F.W., Benndorf, K., Chemical synthesis and biological activity of novel brominated 7-deazaadenosine-3',5'-cyclic monophosphate derivatives, *Bioorganic & Medicinal Chemistry* (2019), doi: https://doi.org/10.1016/j.bmc.2019.03.024

Chemical synthesis and biological activity of novel brominated 7-deazaadenosine-3',5'-cyclic monophosphate derivatives

Marco Lelle[a], Maik Otte[a], Susanne Thon[a], Daniela Bertinetti[b], Friedrich W. Herberg[b], Klaus Benndorf[a]*

[a] Institute of Physiology II, University Hospital Jena, Kollegiengasse 9, 07743 Jena, Germany

[b] Department of Biochemistry, University of Kassel, Heinrich-Plett-Straße 40, 34132 Kassel, Germany

*corresponding author

Keywords:

cAMP derivatives, CNG and HCN channels, protein kinase A, Epac1 and Epac2

Abstract:

Synthetic derivatives of cyclic adenosine monophosphate, such as halogenated or other more hydrophobic analogs, are widely used compounds, to investigate diverse signal transduction pathways of eukaryotic cells. This inspired us to develop cyclic nucleotides, which exhibit chemical structures composed of brominated 7-deazaadenines and the phosphorylated ribosugar. The synthesized 8-bromo- and 7-bromo-7-deazaadenosine-3',5'-cyclic monophosphates rank among the most potent activators of cyclic nucleotide-regulated ion channels as well as cAMP-dependent protein kinase. Moreover, these substances bind tightly to exchange proteins directly activated by cAMP.

1. Introduction:

Cyclic adenosine monophosphate (cAMP) is an important second messenger produced by adenylyl cyclases and plays a fundamental role in many biological processes of eukaryotic cells.[1,2] Signal transduction via cAMP occurs intracellularly through its target molecules, cyclic nucleotide-regulated ion channels, cAMP-dependent protein kinases (PKAs) and exchange proteins directly activated by cAMP (Epacs), upon binding of first messengers, such as hormones or neurotransmitters, to receptors in the cell membrane.[3-7] These target molecules share a highly conserved structural domain, the cyclic nucleotide-binding domain (CNBD), which is involved in the interaction of the protein with cAMP.[8] To study the structure and function of these target proteins, various cyclic nucleotide derivatives with specific properties, including high binding affinity, hydrolytic stability, the ability to permeate the plasma membrane or a selectivity for the different CNBDs, are widely applied.[9-11] The brominated cAMP derivative 8-bromoadenosine-3',5'-cyclic monophosphate (8Br-cAMP) and 7-deazaadenosine-3',5'-cyclic monophosphate (7C-cAMP) display such characteristics

(Figure 1). 8Br-cAMP is a cell-permeable lipophilic analog that efficiently activates cAMP-dependent protein kinases as well as ion channels in many biological systems.[12-14] Moreover, 8Br-cAMP exhibits an increased stability against hydrolysis by different phosphodiesterases, compared to the natural nucleotide.[15] Substitution of the nitrogen atom with a hydrocarbon motif in 7C-cAMP renders the molecule also more lipophilic and restricts hydrogen bonding.[16] This substance has already shown superior binding to numerous target proteins of cAMP. Mechanistically, this can be attributed to stronger interactions with the hydrophobic environment of the binding pocket.[17,18] However, a molecule containing both the bromination and the deaza motif has never been investigated. Such a substance would be promising because the properties of the precursor molecules could be potentially combined or even enhanced. Furthermore, a higher target specificity of such a novel brominated 7-deazaadenosine-3',5'-cyclic monophosphate derivative could help to get deeper insights into particular signaling pathways.

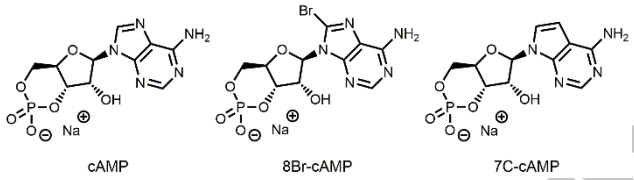

Figure 1: Chemical structures of adenosine-3',5'-cyclic monophosphate (cAMP) and the corresponding derivatives 8Br-cAMP as well as 7C-cAMP.

In the present work, we introduce the synthesis of 8-bromo-7-deazaadenosine-3',5'-cyclic monophosphate (8Br-7C-cAMP) and its 7-brominated analog (7Br-7C-cAMP). This substitution pattern is typically incompatible with the natural nucleotide due to the presence of the nitrogen atom in the purine ring system. To evaluate the potency of the unknown brominated cyclic nucleotides, the effect of the compounds on various cyclic nucleotide-regulated ion channels, cAMP-dependent protein kinase and exchange proteins directly activated by cAMP is examined and compared to the parent nucleotides. In the course of this study, activation of ion channels and PKA is investigated electrophysiologically and by a spectrophotometric assay, respectively. To assess the binding strength to Epac proteins, a competition assay is conducted, where a high-affinity fluorescent probe is displaced by the applied nucleotide.

2. Results and discussion:

2.1 Nucleotide synthesis:

The brominated variants of 7C-cAMP were synthesized from their corresponding halogenated nucleobases by glycosylation and subsequent phosphorylation (Scheme 1). Such a synthesis route is more suitable than the direct halogenation of 7C-cAMP, since the bromination of 7-deazaadenine with *N*-bromosuccinimide at room temperature occurs

exclusively at the 7-position, which has been conducted in our laboratory. As a consequence the 8-bromo derivative would be difficult to access under mild reaction conditions.

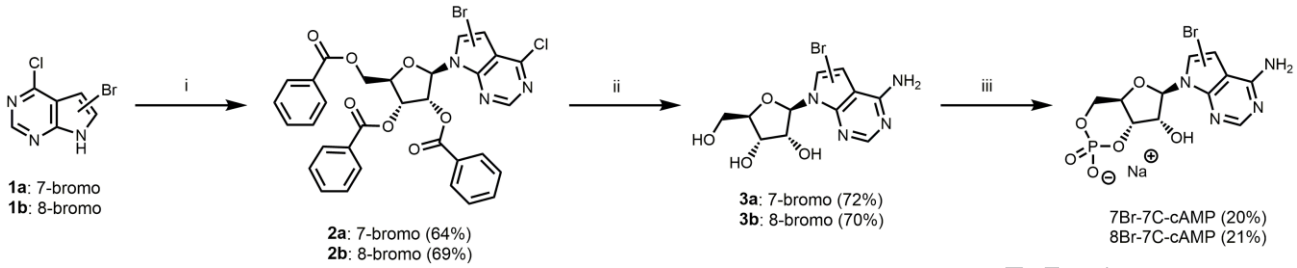

Scheme 1: Synthesis of brominated 7-deazaadenosine-3',5'-cyclic monophosphate derivatives. Reagents and conditions: (i) 1. *N*,*O*-bis(trimethylsilyl)acetamide (1.2 equiv.), acetonitrile, argon, room temperature, 15 min 2. 1-*O*-acetyl-2,3,5-tri-*O*-benzoyl-β-D-ribofuranose (1.2 equiv.), trimethylsilyl trifluoromethanesulfonate (1.2 equiv.), acetonitrile, argon, 80 °C, 2 h; (ii) 7 M ammonia, methanol, 100 °C, 4 h; (iii) 1. phosphorus oxychloride (2 equiv.), trimethyl phosphate, argon, 0 °C, 1 h 2. 0.08 M potassium hydroxide, water/acetonitrile (2:3), room temperature. Yields are given in parentheses.

The initial step was the glycosylation of the brominated nucleobases **1a** and **1b**. This step was carried out via a one-pot procedure of the silyl-Hilbert-Johnson reaction under Vorbrüggen conditions, which is typically employed for 7-halogenated 7-deazapurines.[19,20] The utilization of 1-*O*-acetyl-2,3,5-tri-*O*-benzoyl-β-D-ribofuranose yielded almost entirely the desired β-anomers of the protected nucleosides (**2a**, **2b**). It is widely accepted that the halogenation at the 7-position is a prerequisite for the efficient glycosylation, whereas non-halogenated 7-deazapurine bases nearly resist the modification with the ribosugar under the same reaction conditions.[20,21] If the electron withdrawing substituent is solely at the 8-position, has never been investigated so far. Our results demonstrate that 8-bromo-6-chloro-7-deazapurine yields the protected nucleoside in an efficient way as well. Afterwards, the nucleosides were deprotected with 7 M methanolic ammonia at 100 °C to obtain the compounds **3a** and **3b** in high yield. Thereby, the 6-amino group was generated too.[19,22] The final step was the preparation of the cyclic nucleotides directly from their corresponding nucleosides. This reaction was performed by a modified version of a procedure that is established for several decades.[23,24] To carry out the phosphorylation, the deprotected nucleosides were reacted in trimethyl phosphate with a small excess of phosphorus oxychloride under anhydrous conditions. Subsequently, the obtained reaction mixtures were added to a large amount of aqueous potassium hydroxide in acetonitrile, to achieve cyclization. Before the isolation of the brominated cyclic nucleotides by liquid chromatography, low molecular weight impurities were removed through dialysis against water. The sodium salts of the desired nucleotides were achieved via the addition of a 0.1 M sodium hydrogen carbonate solution, to yield 7Br-7C-cAMP and 8Br-7C-cAMP. These newly synthesized halogenated 7-deazaadenosine-3',5'-cyclic monophosphate derivatives display

an unusual and non-natural scaffold, which is more hydrophobic than the one from its parent nucleotide cAMP.

2.2 Activation of cyclic nucleotide-regulated ion channels:

Cyclic nucleotide-gated (CNG) and hyperpolarization-activated cyclic nucleotide-modulated (HCN) channels belong to the same superfamily of tetrameric ion channels.[3] Nevertheless, their function is remarkably different, CNG channels elicit receptor potentials in olfaction and vision, whereas HCN channels serve as electrical pacemaker in special neurons and cardiomyocytes.[25-28] However, both types of channels are activated by the binding of cyclic nucleotides, such as cAMP, to the CNBD, although HCN channels require a sufficiently hyperpolarizing membrane voltage as primary activating stimulus. Numerous cyclic nucleotide derivatives with diverse substitutions in different positions of the purine ring have been shown to generate an enhanced apparent affinity in CNG and HCN channels as compared to the natural cyclic nucleotides, among them also the lipophilic analogs of cAMP, 7C-cAMP and 8Br-cAMP.[17,29-32]

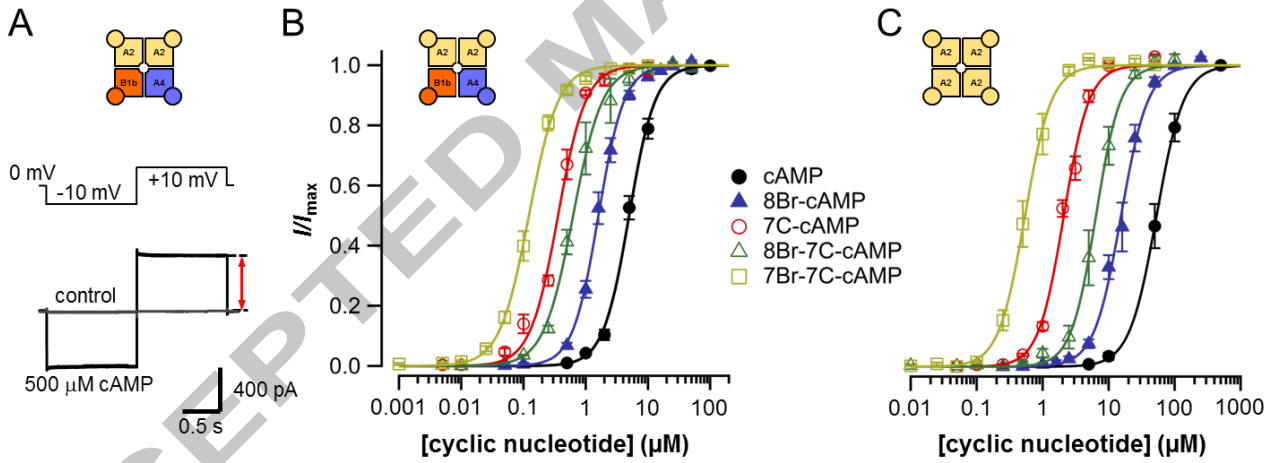

Figure 2: Effect of the novel brominated deaza nucleotides on olfactory channels. (A) Voltage protocol and CNGA2:CNGA4:CNGB1b current evoked by cAMP. The current amplitude was measured at the end of the pulse to +10 mV (red arrow). (B) Concentration-activation relationships for heterotetrameric CNGA2:CNGA4:CNGB1b channels with the five agonists specified in the inset. (C) Concentration-activation relationships for homotetrameric CNGA2 channels with the same agonists. Data points were fitted with Equation 1 (experimental section), yielding the EC_{50} and H values provided by Table 1.

In the present study we investigated the effect of the novel brominated deaza nucleotides on three different types of ion channels by using the patch clamp technique and compared the data with those obtained for the precursor nucleotides. In a first approach we tested the effect of the substances on olfactory CNG channels of natural composition, which are composed of two CNGA2 subunits, one CNGA4 subunit and one CNGB1b subunit.[33] The currents were measured in inside-out patches at +10 mV, following the voltage protocol

indicated in the inset of Figure 2 A. As cAMP, 8Br-cAMP and 7C-cAMP, the two new derivatives 8Br-7C-cAMP and 7Br-7C-cAMP produced robust currents. To determine the potency and efficiency of the compounds, full concentration-activation relationships were determined ~~by applying a series of concentrations for each substance~~ (Figure 2 B). These relationships were fitted by Equation 1 (experimental section), yielding the concentration of half maximum activation, EC_{50}, and the Hill coefficient, H (Table 1). The maximum currents were normalized with respect to the current at saturating cAMP (500 µM). As expected, compared to cAMP the potency was increased by 8Br-cAMP and further by 7C-cAMP. Notably, the potency of both 7Br-7C-cAMP as well as 8Br-7C-cAMP was even higher than that of 7C-cAMP and the potency of 7Br-7C-cAMP exceeded that of 8Br-7C-cAMP. Moreover, all compounds generated at saturating concentrations maximum efficiency with regard to cAMP. All Hill coefficients were approximately similar.

Table 1: EC_{50} of the different agonists and H values derived from the concentration-activation relationships in CNG channels (n represents the number of measurements).

Compound	Heterotetrameric CNGA2:A4:B1b channels			Homotetrameric CNGA2 channels		
	EC_{50} (µM)	H	n	EC_{50} (µM)	H	n
cAMP	4.98 ± 0.15	2.08 ± 0.12	7	53.1 ± 0.6	2.12 ± 0.06	4
8Br-cAMP	1.60 ± 0.03	2.10 ± 0.08	7	15.4 ± 0.5	2.14 ± 0.14	7
7C-cAMP	0.36 ± 0.02	1.95 ± 0.17	4	2.08 ± 0.08	2.27 ± 0.19	6
8Br-7C-cAMP	0.63 ± 0.02	1.83 ± 0.11	5	6.40 ± 0.13	2.32 ± 0.10	6
7Br-7C-cAMP	0.12 ± 0.002	1.84 ± 0.05	7	0.54 ± 0.01	2.17 ± 0.09	7

Afterwards, we studied the effect of the five compounds on homotetrameric CNGA2 channels, which are known to be significantly less sensitive to cAMP as compared to heterotetrameric channels.[34] The results show that the sequence of potency among the agonists was fully preserved. Noticeably, the gain in potency for the most effective agonist, 7Br-7C-cAMP, was even higher as compared to heterotetrameric channels (Figure 2 C and Table 1). Again, all substances were fully efficient at saturating concentrations and the Hill coefficients were approximately similar. This suggests that the binding sites of the CNGA4 and CNGB1b subunit in the heterotetrameric channels function in a similar manner than those of the CNGA2 subunits. Together, these results demonstrate that the novel brominated deaza nucleotides are highly potent and effective agonists in hetero- and homotetrameric olfactory CNG channels.

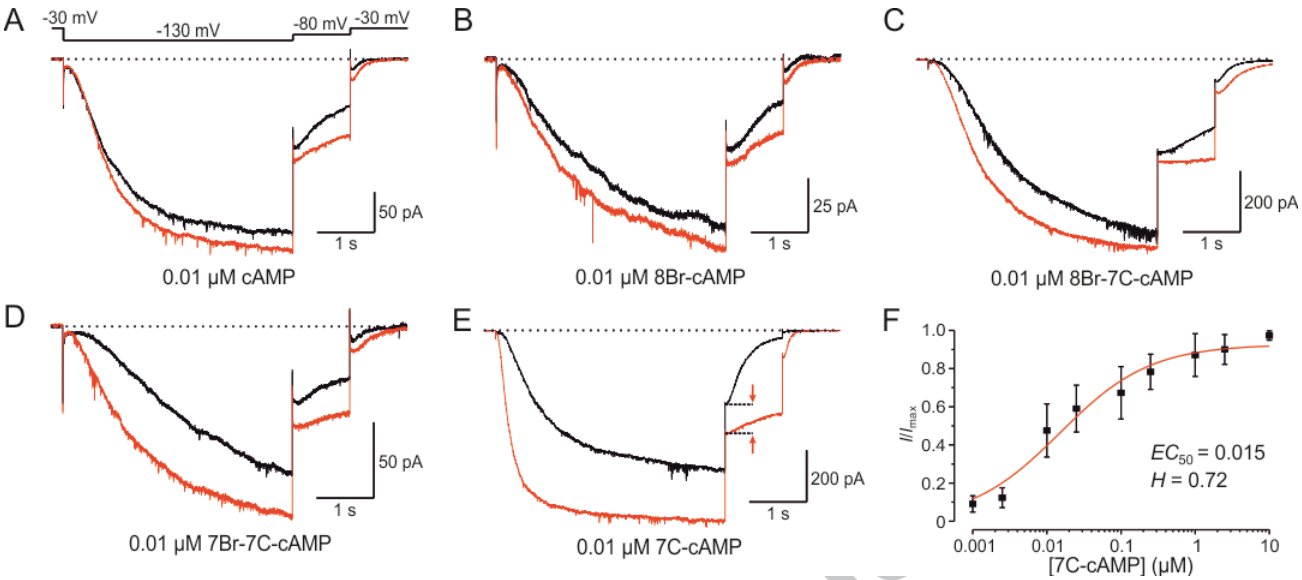

Figure 3: Activation of HCN2 channels by the novel brominated deaza nucleotides. The novel brominated deaza nucleotide agonists (C, D) activate the channels similarly as the known agonists (A, B, E) by both accelerating the activation speed and enhancing the current amplitude at the end of the hyperpolarizing pulses. (F) Representative concentration-activation relationship in HCN2 channels with 7C-cAMP as agonist, the most potent binder in HCN2 channels.[17] The amplitude of the current was determined at -80 mV (red arrows in E) and related to the current with saturating cAMP (I_{max}). The indicated parameters were obtained by fitting Equation 1 (experimental section).

We further tested whether or not our agonists activate also structurally related homotetrameric HCN2 channels. These measurements were performed in inside-out patches as well. The channels were activated from a holding potential of -30 mV by a hyperpolarizing voltage pulse to -130 mV, followed by a short pulse to -80 mV (inset in Figure 3 A). The recordings were performed under control conditions first and then in the presence of an effective concentration of the respective agonist. As typical for cAMP, all substances had a dual effect, they accelerated the current and increased the amplitude at the end of the hyperpolarizing pulse (Figure 3 A-E). For the most effective known binder in isolated monomeric CNBDs of HCN2 channels, 7C-cAMP, a full concentration-activation relationship was determined, to point out that this and also the related compounds are efficient activators in full channels (Figure 3 F).[17] Half-maximum activation was determined to 15 nM. It should be noted, however, that the degree of determinateness in these measurements was inferior as compared to that in CNG channels because of a higher natural variability of HCN channel currents. This finding is also supported by the bigger error bars, compared to those in the diagrams of Figure 2 B and C. Therefore, the Hill coefficient in Figure 3 F should be considered with caution. Despite these limitations, the results show that the novel brominated deaza nucleotides are also highly effective substances to activate structurally related HCN2 channels.

2.3 Activation of cAMP-dependent protein kinase:

Another important target protein of cAMP and its synthetic derivatives in eukaryotic cells is the cAMP-dependent protein kinase (PKA), which regulates cell division, metabolism and apoptosis.[35] Two regulatory (R) and two catalytic (C) subunits form the inactive state of PKA, the heterotetrameric holoenzyme. PKA holoenzymes occur in different isoforms named in respect to their respective R-subunit. The human R-subunits are divided into four isoforms - RIα, RIβ, RIIα and RIIβ - which differ in biochemical characteristics and cellular distribution.[36] However, the α-isoforms are more abundant and are ubiquitously expressed. In the classical concept of PKA activation, four molecules of cAMP bind cooperatively to the CNBDs of the two R-subunits of the holoenzyme. This induces the release of the C-subunits into their catalytically active form, which enables them to phosphorylate nearby substrates.[37] Yet, this concept has been modified recently, using high resolution imaging.[38]

Within the scope of this study, we tested the effect of the aforementioned synthetic cyclic nucleotides on the activation of human PKA *in vitro*. For this purpose, the catalytic activity of PKA was measured in dependence of the cyclic nucleotide concentration (Figure 4). Sigmoidal concentration-response fitting of the resulting data sets allowed us to deduce the apparent activation constants (K_{act}) for the respective cyclic nucleotides (Table 2). The K_{act} corresponds to the cyclic nucleotide concentration that induces half-maximal activation of PKA.

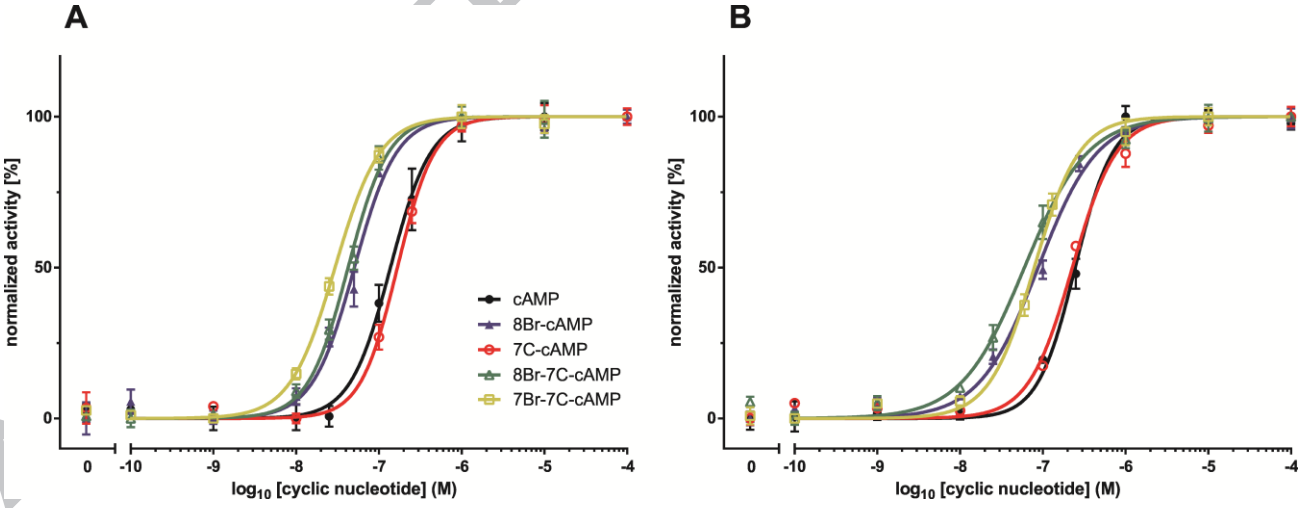

Figure 4: *In vitro* activation of PKA holoenzyme type Iα (A) and IIα (B) by cAMP and synthetic analogs. Inactive PKA holoenzyme was supplemented with increasing concentrations of cyclic nucleotides. The resulting substrate phosphorylation was followed via a photometric assay. Depicted are the data sets of one protein preparation (with each cyclic nucleotide), which are representative for the independent biological duplicates. Each data point depicts the mean ± SEM of at least a technical triplicate. The 0 M data points indicate the PKA activity without nucleotide. Table 2 shows the fit-derived apparent activation constants (K_{act}) of the cyclic nucleotides.

The K_{act} values for PKA were determined in the nanomolar range, in contrast to the micromolar affinity of CNG channels and Epac proteins (see below). Both tested PKA isoforms (Iα and IIα) have nearly identical activation constants for cAMP and 7C-cAMP (Figure 4, Table 2), which is in contrast to CNG channels (Figure 2, Table 1), but in agreement with earlier studies on PKA.[17,39] The observation that 8Br-cAMP activates PKA at a 2 to 4-fold lower cyclic nucleotide concentration than cAMP is also in line with published data and reflects the same tendency as reported above for the CNG channel variants (Figure 2, Table 1).[39] Combining the 8Br substitution with the 7C modification did not alter the activation of PKA: the K_{act} for 8Br-7C-cAMP was nearly the same as for 8Br-cAMP, irrespective of the PKA isoform. However, this finding is in line with the missing effect of the sole 7C substitution on PKA activation and underlines a difference between the CNBDs of PKA and CNG channels with regard to the effect of a deaza modification in position 7 of the adenine moiety.

Interestingly, when the bromo substituent is located at the 7-position of the deaza analog (7Br-7C-cAMP), the cyclic nucleotide has a 2 to 5-times higher activation potency on PKA than cAMP. For PKA IIα this effect correlates with the observations for 8Br-cAMP and 8Br-7C-cAMP. However, for PKA Iα the effect of the 7Br substituent appears to be even stronger than 8Br. It is important to note that the K_{act} of 7Br-7C-cAMP (~30 nM) measured for PKA Iα already approaches the lower detection limit of the assay, because titration effects may occur in this assay with 20 nM PKA used.

Table 2: Apparent activation constants (K_{act}) for PKA holoenzyme type Iα and IIα. Depicted is the mean of the activation constant ± SD of two independent biological experiments. For cAMP and 7C-cAMP similar activation constants have been reported previously.[17,40]

Compound	PKA Iα	PKA IIα
	K_{act} (µM)	K_{act} (µM)
cAMP	0.133 ± 0.006	0.244 ± 0.003
8Br-cAMP	0.056 ± 0.008	0.088 ± 0.001
7C-cAMP	0.199 ± 0.045	0.238 ± 0.015
8Br-7C-cAMP	0.043 ± 0.001	0.072 ± 0.017
7Br-7C-cAMP	0.028 ± 0.002	0.097 ± 0.025

2.4 Cyclic nucleotide binding of exchange proteins directly activated by cAMP:

In humans two isoforms of the exchange proteins directly activated by cAMP (Epac) protein family exist, Epac1 and Epac2~~, encoded by independent genes, Rapgef3 and Rapgef4, respectively~~.[40] As the name implies, Epacs are activated by cAMP and act as nucleotide exchange factor for the Rap subfamily of RAS-like small GTPases (Rap1 and Rap2).[41]

The isoforms display distinct subcellular and tissue-specific localization as well as different physiological functions. Whereas Epac1 is ubiquitously expressed, Epac2 is enriched in the nervous system and endocrine tissues. Dysregulated expression of Epac1 has an influence on several human cancers.[42,43] In contrast, Epac2 plays a major role in the potentiation of glucose induced insulin secretion. Although Epac1 and Epac2 share high structural homology, they differ in the number of CNBDs: Epac1 contains only one cAMP-binding domain (cNBD-B), whereas Epac2 has two (cNBD-A and cNBD-B).[44]

In addition to the experiments with PKA, CNG and HCN channels, we investigated the effects of the novel synthetic cyclic nucleotides on truncated constructs of the two human Epac isoforms ~~(Epac1 and Epac2)~~. Both Epac constructs lack the N-terminal DEP (dishevelled/Egl/pleckstrin) domain, which plays a role in targeting Epac to intracellular membranes.[45,46] Furthermore, the Epac2 construct is deprived of its first CNBD domain, which has a low cAMP affinity and is not involved in the activation process.[40,47] The apparent affinities of the cyclic nucleotides were measured with a fluorescence polarization (FP)-based competition assay, in which the FP signal of the fluorophore (8Fluo-cAMP) decreases in dependence of the Epac binding of the competitor (i.e. the respective cyclic nucleotides). Sigmoidal concentration-response fitting of the resulting data sets (Figure 5) yielded the apparent affinities (EC_{50}) of the cyclic nucleotides for the two isoforms of Epac (Table 3). It is important to note that the EC_{50} value has a different meaning in this context than presented for the CNG and HCN channels, since the FP competition experiment can only indirectly detect the binding of unlabeled cyclic nucleotides. The fit-derived half-maximal concentration is neither a dissociation nor an activation constant. Therefore, the resulting affinity measured is indicated as an effective concentration (*EC*).

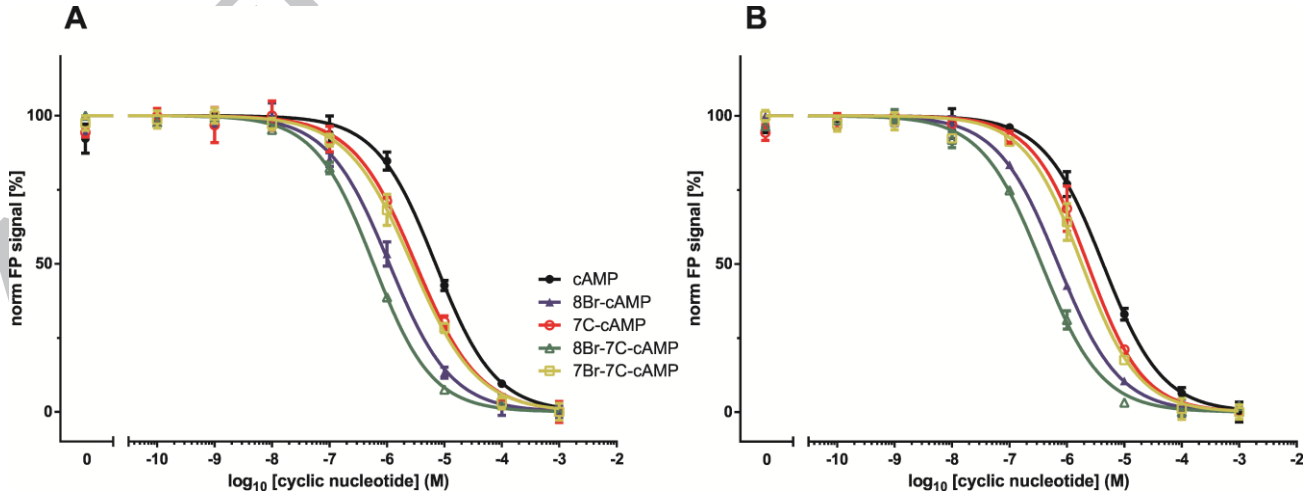

Figure 5: Affinity between Epac and cyclic nucleotides. Representative fluorescence polarization (FP) competition experiments with Epac1 (A) and Epac2 (B) constructs. Increasing concentrations of the cyclic nucleotides were incubated with 1 nM 8Fluo-cAMP and added to 200 nM of the respective Epac protein. Normalized fluorescence polarization was plotted against the competing cyclic nucleotide

concentration. Each data point represents the mean ± SD of triplicates. The most left data points indicate FP signals for the protein incubated without competing nucleotide. The resulting apparent EC_{50} values are provided by Table 3.

For both, Epac1 and Epac2, the apparent affinities of all tested cyclic nucleotides are in the high nanomolar to low micromolar range (Table 3). With apparent cAMP affinities of 5.6 µM for Epac1 and 3.9 µM for Epac2, our data are consistent with previous reports.[40,47-50]

All synthetic analogs in this study showed a higher binding affinity to the Epac isoforms, than the physiologic activator cAMP, which corresponds, in principal, to the observations with CNG channels (Table 1) and to some extent with PKA (Table 2). However, the potency of the bromo substituent and the deaza modification on Epac did not always coincide with the tendencies observed for the other two protein families.

Unlike PKA, both Epac isoforms seem to recognize the sole deaza modification. Nevertheless, the affinities of 7C-cAMP were only increased by a factor of 2 compared to cAMP. 8Br-cAMP, in contrast, even increased the affinity by a factor of 5 compared to unmodified cAMP. This is in line with a published 8-fold increased affinity.[48,50] This effect fits to previous studies on the catalytic activation of Epac1, where the apparent K_{act} was 7-times reduced by the 8Br-cAMP derivative.[49] Notably, among the tested proteins, only CNG channels seem to respond stronger to 7C-cAMP than to 8Br-cAMP. This further substantiates a potential difference in the binding mode, or mechanism respectively, of cyclic nucleotides to CNG channel CNBDs as hypothesized above.

Within the presented set of cyclic nucleotides, we identified the 8Br-7C-cAMP derivative as the most affine binder for Epac where it developed an about 10-times higher binding affinity compared to cAMP. Although this number reflects a similar increase in potency to that observed for CNG channels (Figure 2, Table 1), it is yet remarkable that for both PKA and CNG channels the effect of 7Br-7C-cAMP was even stronger than in the constellation when the bromo substituent was located at the 8-position of the deaza analog. This was not the case for the Epac constructs: here the apparent affinities of 7Br-7C-cAMP were found to be lower than that of 8Br-7C-cAMP and even unchanged compared to 7C-cAMP.

Table 3: Apparent EC_{50} values for Epac1 and Epac2 isoforms derived from a fluorescence polarization competition assay. At least two independent protein preparations were used for each assay and each assay was performed in triplicate.

Compound	Epac1	Epac2
	EC_{50} (µM)	EC_{50} (µM)
cAMP	5.62 ± 0.51	3.87 ± 0.54
8Br-cAMP	1.09 ± 0.01	0.78 ± 0.11
7C-cAMP	2.75 ± 0.59	2.06 ± 0.34

8Br-7C-cAMP	0.53 ± 0.07	0.30 ± 0.07
7Br-7C-cAMP	2.54 ± 0.25	2.36 ± 0.82

3. Conclusions:

In summary, we have presented the synthesis and functional characterization of two novel cyclic nucleotides. Both substances were prepared from their corresponding nucleobases under the same reaction conditions. Thus, we demonstrated that an electron withdrawing bromo substituent in 8-position enables the efficient glycosylation by the established one-pot procedure of the silyl-Hilbert-Johnson reaction under Vorbrüggen conditions as well. The final synthesis step, the phosphorylation and subsequent cyclization, is always challenging, also due to the reaction medium. The utilized trialkyl phosphates cause side reactions and hamper the purification. Our approach employed for the first time dialysis prior to purification, to remove undesired phosphates, which simplified the isolation of the products by liquid chromatography.

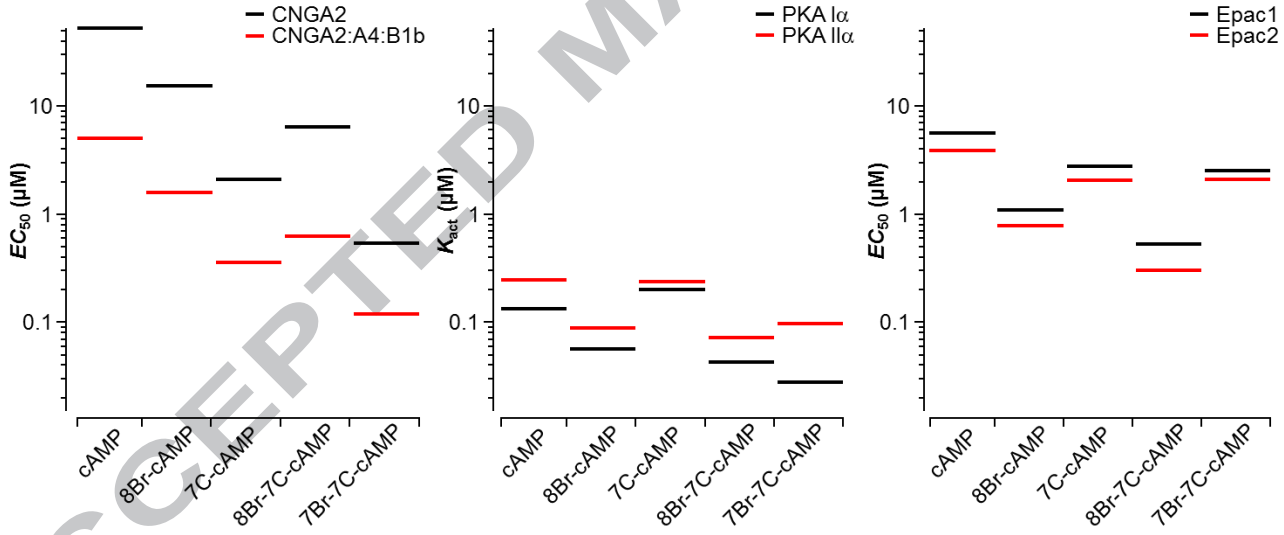

Figure 6: Effect patterns of the investigated cyclic nucleotides in CNG channels, PKA and Epac proteins expressed as EC_{50} and K_{act} values.

The brominated deaza nucleotides are highly efficient activators of cyclic nucleotide-regulated ion channels, 7Br-7C-cAMP is 100-times more potent on homotetrameric CNGA2 channels than natural cAMP. This molecule can also activate PKA Iα in the low nanomolar range. In contrast, Epac proteins respond to this substance like to the natural ligand and 7C-cAMP, but are highly sensitive to 8Br-7C-cAMP. This finding is also supported by Figure 6, which demonstrates that modifications in 7-position do not alter the affinity of the cyclic nucleotide towards Epac1 and Epac2. A similar pattern is observed for PKA, with the exception of 7Br-7C-cAMP and PKA Iα. Astonishingly, the opposite is the case for CNG

channels, where modifications in 7-position induce a bigger effect. Although there is no perfect selectivity of the novel brominated deaza nucleotides for one of their target proteins, there are markedly different patterns of the effects, which can help to learn more about the corresponding CNBDs.

The herein described observation of different cyclic nucleotide recognition patterns by three different protein families could be a valuable starting point for designing cyclic nucleotide analogs, to specifically target only one protein family, while leaving other cAMP-dependent proteins unaffected. Due to the presence of bromo substituents, further modification is enabled. However, for this purpose it would be crucial to obtain structural models of the proteins with the respective analogs bound, to map the key residues for the observed differences in the interaction patterns.

4. Experimental section:

4.1 General information:

Chemicals, including solvents and reagents, were bought from commercial sources and applied without further purification, unless otherwise stated. Cyclic nucleotides were purchased from BIOLOG Life Science Institute (Bremen, Germany). Biotech cellulose ester dialysis tubing (MWCO: 100-500 Da) was obtained from Repligen (Ravensburg, Germany). Thin layer chromatography sheets (ALUGRAM SIL G/UV_{254}) as well as silica gel for column chromatography (0.04-0.063 mm) were ordered from Macherey-Nagel (Düren, Germany) and used with appropriate solvent systems.

Reversed-phase high-performance liquid chromatography (RP-HPLC) was conducted on a Agilent Technologies 1100 Series system (Waldbronn, Germany) with suitable solvent delivery pumps (G1361A), a dual loop autosampler (G2258A) and a multi-wavelength detector (G1365B). Analytical RP-HPLC was carried out on a AppliChrom (Oranienburg, Germany) OTU LipoMare C18 column (250 x 4.6 mm) with 5 µm particle size as stationary phase and a flow rate of 1 mL/min. Purification of the cyclic nucleotides was performed on a AppliChrom OTU LipoMare C18 column (250 x 20 mm) at an appropriate flow rate of 15 mL/min and 5 µm silica as stationary phase. Product fractions were isolated with a fraction collector (G1364C). The applied eluents were 25 mM (pH 7) triethylammonium acetate buffer (A) as well as acetonitrile (B) and were utilized with a linear gradient from 0 min (100% A) to 25 min (75% A). All substances were simultaneously detected at 230 and 260 nm.

UV-Vis absorption spectra were measured on a Analytik Jena SPECORD 250 UV-Vis spectrophotometer (Jena, Germany). Measurements were accomplished at ambient temperature in quartz cuvettes utilizing aqueous solutions of the cyclic nucleotides.

^{1}H, ^{13}C and ^{31}P NMR spectra were recorded at 300 K on a Bruker Avance I 300 MHz spectrometer (Karlsruhe, Germany) or at 297 K on a Bruker Avance III 400 MHz

spectrometer. Chemical shifts are reported in parts per million, relative to the residual solvent signals of DMSO-d_6 and D_2O or DSS-d_6 and phosphoric acid.[51] Coupling constants (*J*) are given in hertz (Hz).

High-resolution electrospray ionization mass spectrometry measurements were carried out on a Bruker Daltonics micrOTOF system (Bremen, Germany), equipped with an automatic syringe pump for sample injection. The standard electrospray ion source was used to generate ions and the instrument was calibrated in the *m*/*z* range 50 to 3000 utilizing an internal calibration standard (Tunemix solution) from Agilent Technologies.

4.2 Chemical syntheses

4.2.1 Synthesis of compound **2a**:

N,*O*-Bis(trimethylsilyl)acetamide (488.2 mg, 586.8 µL, 2.40 mmol) was added to a suspension of 7-bromo-6-chloro-7-deazapurine (464.9 mg, 2.00 mmol) in 20 mL dry acetonitrile. Afterwards, the solution was stirred for 15 min at room temperature in an argon atmosphere, followed by the addition of 1-*O*-acetyl-2,3,5-tri-*O*-benzoyl-β-D-ribofuranose (1.21 g, 2.40 mmol) and trimethylsilyl trifluoromethanesulfonate (533.4 mg, 434.4 µL, 2.40 mmol). The reaction mixture was heated for 2 h at 80 °C under argon with vigorous stirring. After glycosylation, the solution was left to cool down and diluted with 400 mL ethyl acetate. The organic phase was sequentially washed twice with a saturated sodium hydrogen carbonate solution and brine. Subsequently, the organic layer was dried with magnesium sulfate and the solvent was removed under vacuum, to afford the crude nucleoside. Purification by column chromatography on silica gel with hexane/ethyl acetate (2:1) as eluent yielded the product as colorless solid (864.0 mg, 1.28 mmol, 64%). ^{1}H NMR (300 MHz, DMSO-d_6) δ 8.62 (1H, s), 8.32 (1H, s), 8.00-7.84 (6H, m), 7.69-7.61 (3H, m), 7.54-7.40 (6H, m), 6.73 (1H, d, *J* = 5.0 Hz), 6.32-6.28 (1H, m), 6.16-6.11 (1H, m), 4.90-4.85 (1H, m), 4.84-4.65 (2H, m); ^{13}C NMR (75 MHz, DMSO-d_6) δ 165.4, 164.7, 164.5, 151.4, 151.0, 150.3, 134.0, 133.9, 133.6, 129.4, 129.4, 129.3, 129.2, 129.2, 128.8, 128.6, 128.2, 114.9, 88.1, 86.6, 79.3, 73.5, 70.6, 63.4; HRMS (ESI): *m*/*z* calcd for $C_{32}H_{24}BrClN_3O_7$ $[M + H]^+$ 676.0481, found 676.0489

4.2.2 Synthesis of compound **2b**:

This nucleoside derivative was prepared according to the synthesis of **2a** with 8-bromo-6-chloro-7-deazapurine (464.9 mg, 2.00 mmol), to afford the product as colorless solid (931.5 mg, 1.38 mmol, 69%). ^{1}H NMR (300 MHz, DMSO-d_6) δ 8.55 (1H, s), 7.97-7.84 (6H, m), 7.70-7.60 (3H, m), 7.53-7.40 (6H, m), 7.10 (1H, s), 6.72-6.63 (1H, m), 6.50 (1H, d, *J* = 3.8 Hz), 6.45-6.35 (1H, m), 4.95-4.87 (1H, m), 4.84-4.55 (2H, m); ^{13}C NMR (75 MHz, DMSO-d_6) δ 165.3, 164.7,164.6, 150.8, 150.8, 150.0, 134.0, 133.9, 133.5, 129.4, 129.3, 129.2, 129.1,

128.8, 128.7, 128.6, 128.5, 128.3, 118.2, 117.6, 103.5, 88.3, 78.6, 72.8, 69.9, 62.4; HRMS (ESI): *m*/*z* calcd for $C_{32}H_{23}BrClN_3NaO_7$ $[M + Na]^+$ 698.0300, found 698.0309

4.2.3 Synthesis of compound **3a**:

The protected nucleoside **2a** (473.8 mg, 700 µmol) was suspended in 30 mL 7 M ammonia in methanol and heated at 100 °C for 4 h in a sealed reaction vessel with stirring. After that, the solution was cooled to ambient temperature and the solvent was evaporated under reduced pressure. The obtained residue was purified by silica gel column chromatography using dichloromethane/methanol (9:1) as eluent, to yield the product as colorless solid (174.0 mg, 504 µmol, 72%). ^{1}H NMR (300 MHz, DMSO-d_6) δ 8.10 (1H, s), 7.65 (1H, s), 6.82 (2H, br s), 6.04 (1H, d, *J* = 6.2 Hz), 5.35 (1H, d, *J* = 6.5 Hz), 5.25-5.07 (2H, m), 4.41-4.29 (1H, m), 4.12-4.02 (1H, m), 3.93-3.83 (1H, m), 3.67-3.47 (2H, m); ^{13}C NMR (75 MHz, DMSO-d_6) δ 157.0, 152.4, 149.6, 121.8, 101.1, 86.8, 86.7, 85.2, 73.9, 70.5, 61.5; HRMS (ESI): *m*/*z* calcd for $C_{11}H_{14}BrN_4O_4$ $[M + H]^+$ 345.0193, found 345.0198

4.2.4 Synthesis of compound **3b**:

This nucleoside derivative was prepared according to the synthesis of **3a** with **2b** (464.9 mg, 700 µmol), to afford the product as colorless solid (169.1 mg, 490 µmol, 70%). ^{1}H NMR (300 MHz, DMSO-d_6) δ 8.02 (1H, s), 7.28 (2H, br s), 6.80 (1H, s), 5.85 (1H, d, *J* = 6.8 Hz), 5.77-5.69 (1H, m), 5.32 (1H, d, *J* = 6.5 Hz), 5.18-5.04 (2H, m), 4.21-4.13 (1H, m), 3.97-3.90 (1H, m), 3.71-3.46 (2H, m); ^{13}C NMR (75 MHz, DMSO-d_6) δ 156.6, 151.5, 149.6, 109.1, 103.9, 102.9, 90.0, 86.1, 71.2, 70.9, 62.4; HRMS (ESI): *m*/*z* calcd for $C_{11}H_{14}BrN_4O_4$ $[M + H]^+$ 345.0193, found 345.0195

4.2.5 Synthesis of compound 7Br-7C-cAMP:

Compound **3a** (86.3 mg, 250 µmol) was dried in a high vacuum prior to phosphorylation and dissolved in 1.5 mL freshly distilled trimethyl phosphate by heating. Afterwards, freshly distilled phosphorus oxychloride (76.7 mg, 46.5 µL, 500 µmol) was added and the reaction mixture was stirred in an ice bath for 1 h under argon. Subsequently, the solution was poured into 30 mL 0.08 M potassium hydroxide in water/acetonitrile (2:3) with stirring and neutralized by the addition of 1 M hydrochloric acid. The volume was reduced and the residue was diluted with 100 mL 0.1 M sodium hydrogen carbonate. Then, the solution was dialyzed against water and freeze dried. The obtained solid was taken up in 25 mM triethylammonium acetate buffer and the hydrolyzed acid chloride was isolated by RP-HPLC. The solvent of the collected fractions was removed under reduced pressure and the solid was further desiccated in a high vacuum. After that, the residue was dissolved in a small amount of 0.1 M sodium hydrogen carbonate, dialyzed against water and lyophilized, to afford the colorless

product as sodium salt (21.4 mg, 50 µmol, 20%). UV-Vis (H_2O) λ_{max} (ε) = 278 nm (7750 M^{-1} cm^{-1}); ^1H NMR (400 MHz, D_2O) δ 8.01 (1H, s), 7.27 (1H, s), 6.20 (1H, s), 4.63-4.46 (3H, m), 4.34-4.25 (2H, m); ^{13}C NMR (75 MHz, D_2O) δ 156.7, 152.2, 148.1, 121.4, 101.6, 91.0, 89.1, 77.7 (d, *J* = 4.7 Hz), 72.5 (d, *J* = 7.9 Hz), 71.3 (d, *J* = 4.2 Hz), 67.4 (d, *J* = 6.7 Hz); ^{31}P NMR (162 MHz, D_2O) δ -1.65; HRMS (ESI): *m*/*z* calcd for $C_{11}H_{11}BrN_4O_6P$ [M - Na]$^-$ 404.9605, found 404.9602

4.2.6 Synthesis of compound 8Br-7C-cAMP:

This nucleotide derivative was prepared according to the synthesis of 7Br-7C-cAMP with **3b** (86.3 mg, 250 µmol), to afford the product as colorless solid (22.5 mg, 53 µmol, 21%). UV-Vis (H_2O) λ_{max} (ε) = 277 nm (14050 M^{-1} cm^{-1}); ^1H NMR (400 MHz, D_2O) δ 8.09 (1H, s), 6.63 (1H, s), 6.17 (1H, d, *J* = 1.4 Hz), 5.34-5.25 (1H, m), 5.10-5.03 (1H, m), 4.54-4.42 (1H, m), 4.33-4.25 (1H, m), 4.24-4.15 (1H, m); ^{13}C NMR (75 MHz, D_2O) δ 155.9, 151.8, 150.0, 109.0, 104.0, 103.8, 92.9, 76.9 (d, *J* = 4.3 Hz), 71.5 (d, *J* = 4.4 Hz), 71.0 (d, *J* = 8.0 Hz), 67.2 (d, *J* = 7.0 Hz); ^{31}P NMR (162 MHz, D_2O) δ -1.45; HRMS (ESI): *m*/*z* calcd for $C_{11}H_{11}BrN_4O_6P$ [M - Na]$^-$ 404.9605, found 404.9596

4.3 Molecular biology and heterologous expression of CNG and HCN channels:

The subunits CNGA2 (accession No. AF126808), CNGA4 (accession No. U12623) and CNGB1b (accession No. AF068572) of rat olfactory channels as well as of mouse HCN2 channels (NM008226) were subcloned prior to the T7 promoter of pGEMHEnew. The respective cRNAs were produced by using the mMESSAGE mMACHINE T7 Kit (Ambion, Austin, TX, USA).

Oocytes of *Xenopus laevis* were harvested either surgically under anesthesia (0.3% 3-aminobenzoic acid ethyl ester) from female adults or purchased from Ecocyte® (Castrop-Rauxel, Germany). The procedures had approval from the authorized animal ethical committee of the Friedrich Schiller University Jena and were carried out in accordance with the approved guidelines.

The oocytes were incubated for 105 min in Ca^{2+}-free Barth's medium containing collagenase A (3 mg/ml; Roche, Grenzach-Wyhlen, Germany) and (in mM) 82.5 NaCl, 2 KCl, 1 MgCl 2, and 5 Hepes, pH 7.4. Oocytes at stages IV and V were injected with 50-130 ng cRNA encoding either CNGA2, CNGA2:CNGA4:CNGB1b (2:1:1 ratio) or HCN2 channels either by hand or by means of an injection robot (RoboInject®). The injected oocytes were then incubated at 18 °C for up to 6 days in Barth's solution containing (in mM) 84 NaCl, 1 KCl, 2.4 $NaHCO_3$, 0.82 $MgSO_4$, 0.41 $CaCl_2$, 0.33 $Ca(NO_3)_2$, 7.5 TRIS, cefuroxime (4.0 µg×ml^{-1}), penicillin/streptomycin (100 µg×ml^{-1}), pH 7.4.

4.4 Electrophysiology:

Macroscopic currents containing hundreds to several thousand of channels were recorded from inside-out patches of the oocytes by the patch-clamp technique. The patch pipettes were pulled from quartz tubing (P-2000, Sutter Instrument, Novato, USA) with an outer and inner diameter of 1.0 and 0.7 mm (VITROCOM, New Jersey, USA). The corresponding pipette resistance was 0.9-2.3 MΩ. The bath and pipette solution contained (in mM): 150 KCl, 1 EGTA, 5 Hepes (pH 7.4 with KOH). Recording was performed by an Axopatch 200B amplifier (Axon Instruments, Foster City, CA, USA). Electrophysiology was controlled by the Patchmaster-software (HEKA Elektronik Dr. Schulze GmbH, Lambrecht, Germany). The sampling rate was 5 kHz and the filter implemented in the amplifier (4-pole Bessel) was set to 2 kHz. Measurements in HCN2 channels were begun 3.5 min after patch excision to minimize channel run down during the measurement.[52] The solutions with the different ligand concentrations to be tested were applied via a multi-barrel device to the patches with a flow rate of 0.8 to 1.2 mL/min. All experiments were carried out at room temperature.

4.5 Fitting steady-state concentration-activation relationships (CNG and HCN channels):

Concentration-activation relationships were fitted with the Igor software® by the following formula (Equation 1):

$$I/I_{max} = 1/(1+(EC_{50}/[\text{nucleotide}])^{H}) \quad (1)$$

where I is the actual current amplitude and I_{max} the maximum current amplitude at saturating concentration specified for each cyclic nucleotide derivative separately. EC_{50} is the concentration generating the half maximum current and H the Hill coefficient. Errors are given as mean ± s.e.m.

4.6 Expression and purification of catalytic and regulatory subunits of PKA:

The human catalytic subunit (Cα1) and the two main human regulatory subunits (RIα, RIIα) of PKA were recombinantly expressed in *E. coli*, purified via Sp-8-AEA-cAMPS agarose and characterized as described previously.[53] *In vitro* formation of PKA holoenzymes (i.e. association of the heterotetramer R_2C_2) was performed as reported.[40]

4.7 PKA activity assay:

The cyclic nucleotide-dependent activity of PKA was monitored *in vitro*, using a coupled spectrophotometric assay described by Cook *et al.*.[54] Each substrate phosphorylation event catalyzed by an active PKA C-subunit produces one ADP molecule, which is regenerated to ATP by a pyruvate kinase, in turn releasing pyruvate. Pyruvate is converted to lactic acid by a lactate dehydrogenase under the consumption of $NADH+H^+$. The oxidation of $NADH+H^+$ is stoichiometric with substrate phosphorylation by PKA and can be followed photometrically at

340 nm. The enzyme activity refers to the initial reaction rate (v_0). The concentration of the commonly used synthetic PKA substrate Kemptide (LRRASLG; GeneCust, Dudelange, Luxembourg) was adopted from previous studies (260 µM).[55] The cyclic nucleotide analogs were applied in a concentration range of 100 pM to 1 mM. The concentration of PKA holoenzyme was adapted to the specific activity of the catalytic subunit preparation (15 U/mg active catalytic subunit), employing approximately 10 nM of holoenzyme in the assay. All data points were obtained at least in triplicates and analyzed with GraphPad Prism 6.01 (GraphPad Software Inc., La Jolla, California). For each cyclic nucleotide, v_0 was normalized to the smallest (0%) and largest (100%) mean of the replicates. The apparent activation constants (K_{act}) were determined by fitting the concentration-dependent normalized activity with a sigmoid dose-response model (where top and bottom values were constrain to 100% and 0%, respectively). In addition to the technical triplicate of each data point, the full data set of each cyclic nucleotide analog was statistically verified by a biological duplicate, i.e. with independent protein expressions, purifications and PKA holoenzyme formations.

4.8 Expression and purification of Epac constructs:

Expression plasmids with human His-tagged Epac1 157-881 (referred to as Epac1) were transformed into *E. coli* TP2000 Δcya (gift from C. Kim, Baylor College of Medicine, Houston, TX, USA) by electroporation. 20 mL seed cultures were grown overnight at 37 °C and 180 rpm. Main cultures were inoculated 1:500 with seed culture and incubated at room temperature and 180 rpm until an OD_{600} of 0.6-0.8 was reached. Expression was induced by adding 400 µM isopropyl β-D-1-thiogalactopyranoside and proteins were expressed overnight at room temperature. Cells were harvested by centrifugation at 9,000 xg for 20 min and cell pellets were stored at -20 °C until they were further processed.

Cell pellets were resuspended in buffer A (20 mM NaH_2PO4, 300 mM $NaCl_2$, 5 mM 2-mercaptoethanol, pH8) containing cOmplete EDTA-free protease inhibitor cocktail (Roche) and 1 mM PMSF. After homogenization, the suspension was lysed by 3 rounds of French pressure cell (Thermo Electron Corp.) treatment, applying a pressure of ~1,000 bar. The cell debris was spun down at 40,000 xg for at least 30 min at 4 °C. The supernatant was passed through a 0.45 µm PVDF syringe-filter (Roth, Karlsruhe, Germany).

The purification was performed at 4°C with following FPLC assembly: ÄKTA purifier UPC 10, fraction collector Frac-920, software Unicorn 5.31 (all GE Healthcare). The filtered supernatant was loaded on a 1 ml Protino Ni-NTA column (Macherey-Nagel) via a superloop (GE Healthcare). The purification was carried out at a flow rate of up to 1 mL/min and a pressure limit of 0.7 MPa. After loading the lysate, the column was washed with 10 column volumes of 20 mM imidazole in buffer A. Subsequently, His-tagged protein was eluted with

gradually increasing imidazole concentrations: from 40 to 250 mM imidazole, linearly distributed over 20 column volumes. 1 mL fractions were collected.

Pooled elution fractions were concentrated and buffer exchanged via Amicon Ultra-15 30K Centrifugal Filter Units (Merck Millipore), 2,500 xg, 50 min. Afterwards, 2 mL of the purified His-tagged Epac1 157-881 were subjected to gel filtration on a Superdex 75 16/60 column (GE Healthcare) in 20 mM MOPS, 150 mM NaCl, 5 mM 2-mercaptoethanol, pH 7 at a flow rate of 2 mL/min and a pressure limit of 0.8 MPa. 2 mL fractions were collected. The column was calibrated using the Gel Filtration Standard (Bio-Rad) according to the manufacturer's protocol. SDS-PAGE was used to monitor protein expression and purification, in order to ensure a homogeneity of ≥95%.

Mus musculus Epac2 ΔDEP (aa 280-998, referred to as Epac2)[56] was kindly provided by H. Rehmann (UMC Utrecht, Netherlands).

Epac concentrations were determined according to a calibration curve with Bovine Serum Albumin (Pierce) using Bradford reagent (Bio-Rad).

4.9 Epac binding assay:

In order to measure the binding affinities of the synthetic cyclic nucleotides, a fluorescence polarization-based competition assay, previously developed for PKA,[57] was adapted to Epac. The concentrations of both protein and 8Fluo-cAMP were fixed, while the concentration of the competing cyclic nucleotide was varied over several orders of magnitude. When 8Fluo-cAMP is bound to the protein, its rotational speed is slowed down in comparison to unbound 8Fluo-cAMP, which can be quantified according to the fluorescence polarization signal.

The FP measurements were performed in 150 mM NaCl, 20 mM MOPS with 0.005% (v/v) CHAPS, pH 7 at room temperature. All data points were obtained in triplicates using a CLARIOstar plate reader (BMG LABTECH). Data point acquisition took place with a rate of 10 s^{-1} at an excitation and emission wavelength of 482 nm and 520 nm, respectively, in black 384 well microtiter plates (BRANDplate, BRAND GMBH + CO KG).

Prior to determination of the binding affinities of the target analogs via a competition assay, the interaction between a fluorescently labeled cAMP analog (8Fluo-cAMP, 8-[[2-[(fluoresceinylthioureido)amino]ethyl]thio]-cAMP, BIOLOG Life Science Institute) and the Epac isoforms was analyzed (supporting information). In this direct assay format, the respective Epac isoform was varied (120 pM to 2 µM), whereas the 8Fluo-cAMP concentration was held constant (1 nM). For the FP competition assay, increasing concentrations of cAMP and target analog (ranging from 100 pM to 1 mM) were mixed with 1 nM 8Fluo-cAMP before addition of the respective Epac isoform. The Epac concentration (200 nM) was adapted to the results of the direct interaction assay, in order to reach ~50% of the maximum FP signal (~100 mPol). The FP measurement was started after 5 minutes of

incubation. For each cyclic nucleotide, the FP signal was normalized to the smallest (0%) and largest (100%) mean of the replicates. Apparent EC_{50} values were calculated by fitting with a nonlinear sigmoid dose-response model (where top and bottom values were constrained to 100% and 0%, respectively) with the software GraphPad Prism 6.01. In addition to the technical triplicate of each data point, a biological duplicate, i.e. with an independent protein expression and purification, statistically verified the full data set of each cyclic nucleotide analog.

Conflicts of interest:

There are no conflicts to declare.

Acknowledgements:

We thank K. Schoknecht, S. Bernhardt, A. Kolchmeier, U. Enke and C. Ranke from the University Hospital Jena as well as M. Hansch and O. Bertinetti from the University of Kassel for excellent technical assistance and L.L. Kailing (University of Kassel) for critically reading and constructive discussions on the manuscript. Moreover, we would like to acknowledge the NMR platform at Friedrich Schiller University Jena for support in NMR spectroscopy as well as the mass spectrometry facility of Professor U.S. Schubert from the Friedrich Schiller University Jena. This work was supported by the Deutsche Forschungsgemeinschaft (TRR 166 ReceptorLight, project A5 to K.B., and He 1818/10 to F.W.H.).

Supplementary data:

Supplementary data contain acquired NMR data, including the corresponding structure assignments, UV-Vis absorption spectra, RP-HPLC chromatograms, high-resolution mass spectra as well as additional information regarding the Epac binding assay. Supplementary data associated with this article can be found, in the online version, at …

References:

1. Beavo JA, Brunton LL. Cyclic nucleotide research - still expanding after half a century. *Nat Rev Mol Cell Biol*. 2002;3:710-718.

2. Bassler J, Schultz JE, Lupas AN. Adenylate cyclases: Receivers, transducers, and generators of signals. *Cell Signal*. 2018;46:135-144.

3. Craven KB, Zagotta WN. CNG and HCN channels: Two peas, one pod. *Annu Rev Physiol*. 2006;68:375-401.

4. Kaupp UB, Seifert R. Cyclic nucleotide-gated ion channels. *Physiol Rev*. 2002;82:769-824.

5. Taylor SS, Zhang P, Steichen JM, Keshwani MM, Kornev AP. PKA: Lessons learned after twenty years. *BBA-Proteins Proteom*. 2013;1834:1271-1278.

6. Bos JL. Epac: a new cAMP target and new avenues in cAMP research. *Nat Rev Mol Cell Biol*. 2003;4:733-738.

7. Schmidt M, Dekker FJ, Maarsingh H. Exchange Protein Directly Activated by cAMP (epac): A Multidomain cAMP Mediator in the Regulation of Diverse Biological Functions. *Pharmacol Rev*. 2013;65:670-709.

8. Berman HM, Ten Eyck LF, Goodsell DS, Haste NM, Kornev A, Taylor SS. The cAMP binding domain: An ancient signaling module. *Proc Natl Acad Sci*. 2005;102:45-50.

9. Poppe H, Rybalkin SD, Rehmann H, Hinds TR, Tang XB, Christensen AE, Schwede F, Genieser H-G, Bos JL, Doskeland SO, Beavo JA, Butt E. Cyclic nucleotide analogs as probes of signaling pathways. *Nat Methods*. 2008;5:277-278.

10. Schwede F, Maronde E, Genieser H-G, Jastorff B. Cyclic nucleotide analogs as biochemical tools and prospective drugs. *Pharmacol Ther*. 2000;87:199-226.

11. Scott SP, Shea PW, Dryer SE. Mapping ligand interactions with the hyperpolarization activated cyclic nucleotide modulated (HCN) ion channel binding domain using a soluble Construct. *Biochemistry*. 2007;46:9417-9431.

12. Bartsch M, Zorn-Kruppa M, Kuhl N, Genieser H-G, Schwede F, Jastorff B. Bioactivatable, membrane-permeant analogs of cyclic nucleotides as biological tools for growth control of C6 glioma cells. *Biol Chem*. 2003;384:1321-1326.

13. Blasic JR, Brown RL, Robinson PR. Phosphorylation of Mouse Melanopsin by Protein Kinase A. *PLoS ONE*. 2012;7.

14. Huang H, Trussell LO. Presynaptic HCN Channels Regulate Vesicular Glutamate Transport. *Neuron*. 2014;84:340-346.

15. Sandberg M, Butt E, Nolte C, Fischer L, Halbrugge M, Beltman J, Jahnsen T, Genieser H-G, Jastorff B, Walter U. Characterization of Sp-5,6-Dichloro-1-Beta-D-Ribofuranosyl-Benzimidazole-3',5'-Monophosphorothioate (Sp-5,6-Dcl-Cbimps) as a Potent and Specific Activator of Cyclic-Amp-Dependent Protein-Kinase in Cell-Extracts and Intact-Cells. *Biochem J*. 1991;279:521-527.

16. Werner K, Schwede F, Genieser H-G, Geiger J, Butt E. Quantification of cAMP and cGMP analogs in intact cells: pitfalls in enzyme immunoassays for cyclic nucleotides. *Naunyn Schmiedebergs Arch Pharmacol*. 2011;384:169-176.

17. Möller S, Alfieri A, Bertinetti D, Aquila M, Schwede F, Lolicato M, Rehmann H, Moroni A, Herberg FW. Cyclic Nucleotide Mapping of Hyperpolarization-Activated Cyclic Nucleotide-Gated (HCN) Channels. *ACS Chem Biol*. 2014;9:1128-1137.

18. Sartiani L, Mannaioni G, Masi A, Romanelli MN, Cerbai E. The Hyperpolarization-Activated Cyclic Nucleotide-Gated Channels: from Biophysics to Pharmacology of a Unique Family of Ion Channels. *Pharmacol Rev*. 2017;69:354-395.

19. Seela F, Peng XH. 7-functionalized 7-deazapurine ribonucleosides related to 2-aminoadenosine, guanosine, and xanthosine: Glycosylation of pyrrolo[2,3-d]pyrimidines with 1-O-acetyl-2,3,5-tri-O-benzoyl-D-ribofuranose. *J Org Chem*. 2006;71:81-90.

20. Seela F, Ming X. 7-Functionalized 7-deazapurine beta-D and beta-L-ribonucleosides related to tubercidin and 7-deazainosine: glycosylation of pyrrolo[2,3-d] pyrimidines with 1-O-acetyl-2,3,5-tri-O-benzoyl-beta-D or beta-L-ribofuranose. *Tetrahedron*. 2007;63:9850-9861.

21. Ingale SA, Leonard P, Seela F. Glycosylation of Pyrrolo[2,3-d]pyrimidines with 1-O-Acetyl-2,3,5-tri-O-benzoyl-β-d-ribofuranose: Substituents and Protecting Groups Effecting the Synthesis of 7-Deazapurine Ribonucleosides. *J Org Chem*. 2018;83:8589-8595.

22. De Ornellas S, Slattery JM, Edkins RM, Beeby A, Baumann CG, Fairlam IJS. Design and synthesis of fluorescent 7-deazaadenosine nucleosides containing pi-extended diarylacetylene motifs. *Org Biomol Chem*. 2015;13:68-72.

23. Genieser H-G, Butt E, Bottin U, Dostmann W, Jastorff B. Synthesis of the 3',5'-Cyclic Phosphates from Unprotected Nucleosides. *Synthesis*. 1989;53-54.

24. Roy B, Depaix A, Perigaud C, Peyrottes S. Recent Trends in Nucleotide Synthesis. *Chem Rev*. 2016;116:7854-7897.

25. Nache V, Wongsamitkul N, Kusch J, Zimmer T, Schwede F, Benndorf K. Deciphering the function of the CNGB1b subunit in olfactory CNG channels. *Sci Rep*. 2016;6.

26. Shuart NG, Haitin Y, Camp SS, Black KD, Zagotta WN. Molecular mechanism for 3:1 subunit stoichiometry of rod cyclic nucleotide-gated ion channels. *Nat Commun*. 2011;2.

27. Peng CH, Rich ED, Varnum MD. Subunit configuration of heteromeric cone cyclic nucleotide-gated channels. *Neuron*. 2004;42:401-410.

28. Thon S, Schmauder R, Benndorf K. Elementary Functional Properties of Single HCN2 Channels. *Biophys J*. 2013;105:1581-1589.

29. Chen L, Xu R, Sun FJ, Xue Y, Hao XM, Liu HX, Wang H, Chen XY, Liu ZR, Deng WS, Han XH, Xie JX, Yung WH. Hyperpolarization-activated cyclic nucleotide-gated (HCN) channels regulate firing of globus pallidus neurons in vivo. *Mol Cell Neurosci*. 2015;68:46-55.

30. V H, Frings S, Wiesner B, Helm S, Kaupp UB, Bendig J. [7-(dialkylamino)coumarin-4-yl]methyl-caged compounds as ultrafast and effective long-wavelength phototriggers of 8-bromo-substituted cyclic nucleotides. *ChemBioChem*. 2003;4:434-442.

31. Otte M, Schweinitz A, Bonus M, Enke U, Schumann C, Gohlke H, Benndorf K. Hydrophobic alkyl chains substituted to the 8-position of cyclic nucleotides enhance activation of CNG and HCN channels by an intricate enthalpy - entropy compensation. *Sci Rep*. 2018;8.

32. Brown RL, Strassmaier T, Brady JD, Karpen JW. The pharmacology of cyclic nucleotide-gated channels: Emerging from the darkness. *Curr Pharm Des*. 2006;12:3597-3613.

33. Bonigk W, Bradley J, Muller F, Sesti F, I B, Ronnett GV, Kaupp UB, Frings S. The native rat olfactory cyclic nucleotide-gated channel is composed of three distinct subunits. *J Neurosci*. 1999;19:5332-5347.

34. Nache V, Zimmer T, Wongsamitkul N, Schmauder R, Kusch J, Reinhardt L, Bonigk W, Seifert R, Biskup C, Schwede F, Benndorf K. Differential Regulation by Cyclic Nucleotides of the CNGA4 and CNGB1b Subunits in Olfactory Cyclic Nucleotide-Gated Channels. *Sci Signal*. 2012;5.

35. Skalhegg BS, Tasken K. Specificity in the cAMP/PKA signaling pathway. Differential expression, regulation, and subcellular localization of subunits of PKA. *Front Biosci*. 2000;5:D678-D693.

36. Soberg K, Skalhegg BS. The Molecular Basis for Specificity at the Level of the Protein Kinase a Catalytic Subunit. *Front Endocrinol*. 2018;9.

37. England JP, Hao YX, Bai LH, Glick V, Hodges HC, Taylor SS, Maillard RA. Switching of the folding-energy landscape governs the allosteric activation of protein kinase A. *Proc Natl Acad Sci*. 2018;115:E7478-E7485.

38. Smith FD, Esseltine JL, Nygren PJ, Veesler D, Byrne DP, Vonderach M, Strashnov I, Eyers CE, Eyers PA, Langeberg LK, Scott JD. Local protein kinase A action proceeds through intact holoenzymes. *Science*. 2017;356:1288-1293.

39. Ogreid D, Ekanger R, Suva RH, Miller JP, Sturm P, Corbin JD, Doskeland SO. Activation of Protein-Kinase Isozymes by Cyclic-Nucleotide Analogs Used Singly or in Combination - Principles for Optimizing the Isozyme Specificity of Analog Combinations. *Eur J Biochem*. 1985;150:219-227.

40. Schwede F, Bertinetti D, Langerijs CN, Hadders MA, Wienk H, Ellenbroek JH, de Koning EJP, Bos JL, Herberg FW, Genieser H-G, Janssen RAJ, Rehmann H. Structure-Guided Design of Selective Epac1 and Epac2 Agonists. *PLoS Biol*. 2015;13:e1002038.

41. Wang PY, Liu ZQ, Chen HY, Ye N, Cheng XD, Zhou J. Exchange proteins directly activated by cAMP (EPACs): Emerging therapeutic targets. *Bioorg Med Chem Lett*. 2017;27:1633-1639.

42. Sun DP, Fang CL, Chen HK, Wen KS, Hseu YC, Hung ST, Uen YH, Lin KY. EPAC1 overexpression is a prognostic marker and its inhibition shows promising therapeutic potential for gastric cancer. *Oncol Rep*. 2017;37:1953-1960.

43. Ichikawa H, Itsumi M, Kajioka S, Maki T, Lee K, Tomita M, Yamaoka S. Overexpression of exchange protein directly activated by cAMP-1 (EPAC1) attenuates bladder cancer cell migration. *Biochem Biophys Res Commun*. 2018;495:64-70.

44. Pereira L, Rehmann H, Lao DH, Erickson JR, Bossuyt J, Chen J, Bers DM. Novel Epac fluorescent ligand reveals distinct Epac1 vs. Epac2 distribution and function in cardiomyocytes. *Proc Natl Acad Sci*. 2015;112:3991-3996.

45. Ponsioen B, Gloerich M, Ritsma L, Rehmann H, Bos JL, Jalink K. Direct Spatial Control of Epac1 by Cyclic AMP. *Mol Cell Biol*. 2009;29:2521-2531.

46. Li S, Tsalkova T, White MA, Mei FC, Liu T, Wang D, Woods VL, Cheng XD. Mechanism of intracellular cAMP sensor Epac2 activation: cAMP-induced conformational changes identified by amide hydrogen/deuterium exchange mass spectrometry (DXMS). *J Biol Chem*. 2011;286:17889-17897.

47. Rehmann H, Das J, Knipscheer P, Wittinghofer A, Bos JL. Structure of the cyclic-AMP-responsive exchange factor Epac2 in its auto-inhibited state. *Nature*. 2006;439:625-628.

48. Christensen AE, Selheim F, de Rooij J, Dremier S, Schwede F, Dao KK, Martinez A, Maenhaut C, Bos JL, Genieser H-G, Doskeland SO. cAMP analog mapping of Epac1 and cAMP kinase - Discriminating analogs demonstrate that Epac and cAMP kinase act synergistically to promote PC-12 cell neurite extension. *J Biol Chem*. 2003;278:35394-35402.

49. Rehmann H, Schwede F, Doskeland SO, Wittinghofer A, Bos JL. Ligand-mediated activation of the cAMP-responsive guanine nucleotide exchange factor Epac. *J Biol Chem*. 2003;278:38548-38556.

50. Dao KK, Teigen K, Kopperud R, Hodneland E, Schwede F, Christensen AE, Martinez A, Dskeland SO. Epac1 and cAMP-dependent protein kinase holoenzyme have similar cAMP affinity, but their cAMP domains have distinct structural features and cyclic nucleotide recognition. *J Biol Chem*. 2006;281:21500-21511.

51. Gottlieb HE, Kotlyar V, Nudelman A. NMR chemical shifts of common laboratory solvents as trace impurities. *J Org Chem*. 1997;62:7512-7515.

52. DiFrancesco D. Characterization of Single Pacemaker Channels in Cardiac Sinoatrial Node Cells. *Nature*. 1986;324:470-473.

53. Bertinetti D, Schweinsberg S, Hanke SE, Schwede F, Bertinetti O, Drewianka S, Genieser H-G, Herberg FW. Chemical tools selectively target components of the PKA system. *BMC Chem Biol*. 2009;9:3.

54. Cook PF, Neville ME, Vrana KE, Hartl FT, Roskoski R. Adenosine Cyclic 3',5'-Monophosphate Dependent Protein-Kinase - Kinetic Mechanism for the Bovine Skeletal-Muscle Catalytic Subunit. *Biochemistry*. 1982;21:5794-5799.

55. Chepurny OG, Bertinetti D, Diskar M, Leech CA, Afshari P, Tsalkova T, Cheng XD, Schwede F, Genieser H-G, Herberg FW, Holz GG. Stimulation of Proglucagon Gene Expression by Human GPR119 in Enteroendocrine L-cell Line GLUTag. *Mol Endocrinol*. 2013;27:1267-1282.

56. Rehmann H, Prakash B, Wolf E, Rueppel A, de Rooij J, Bos JL, Wittinghofer A. Structure and regulation of the cAMP-binding domains of Epac2. *Nat Struct Biol*. 2003;10:26-32.

57. Moll D, Prinz A, Gesellchen F, Drewianka S, Zimmermann B, Herberg FW. Biomolecular interaction analysis in functional proteomics. *J Neural Transm*. 2006;113:1015-1032.

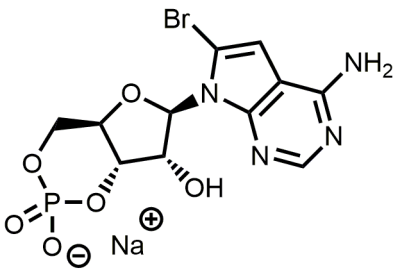

EC_{50} (CNGA2) = 6.40 µM

EC_{50} (CNGA2:A4:B1b) = 0.63 µM

K_{act} (PKA Iα) = 0.043 µM

K_{act} (PKA IIα) = 0.072 µM

EC_{50} (Epac1) = 0.53 µM

EC_{50} (Epac2) = 0.30 µM

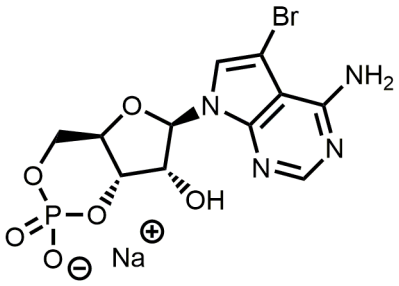

EC_{50} (CNGA2) = 0.54 µM

EC_{50} (CNGA2:A4:B1b) = 0.12 µM

K_{act} (PKA Iα) = 0.028 µM

K_{act} (PKA IIα) = 0.097 µM

EC_{50} (Epac1) = 2.54 µM

EC_{50} (Epac2) = 2.36 µM